

On the formation of protected gold nanoparticles from AuCl_4^- by the reduction using aromatic amines

Chandramouli Subramaniam, Renjis T. Tom and T. Pradeep

Department of Chemistry and Sophisticated Analytical Instrument Facility, Indian Institute of Technology Madras, Chennai 600 036, India (Fax: +91-44-2257-0509/0545; E-mail: pradeep@iitm.ac.in)

Received 23 July 2004; accepted in revised form 4 January 2005

Key words: gold nanoparticles, poly(2-methyl aniline), core-shell nanomaterials, oxidative polymerization, MALDI-MS

Abstract

Amines are used extensively as reductants and subsequent capping agents in the synthesis of metal nanoparticles, especially gold, due to its affinity to nitrogen. Taking 2-methyl aniline as an example, we show that metal reduction is followed by polymerization of the amine, while part of it covers the nanoparticle surface another fraction deposits in the solution. It is found that the oxidative polymerization of the amine goes in step with the formation of gold nanoparticles. The gold nanoparticles thus formed have a mean diameter of 20 nm. The polymerized amine encapsulates the gold nanoparticle forming a robust shell of about 5 nm thickness, making the gold core inert towards mineralizing agents such as chloroform, bromoform, sodium cyanide, benzylchloride, etc. which react with the naked gold nanoparticles. The deposited polymer is largely protonated, taking up protons from the medium during its formation. Similar results have been observed in the case of aniline also. The materials have been fully characterized by spectroscopy and microscopy.

Introduction

Metal nanoparticles have been known to exhibit properties sensitive to their immediate environment and hence there has been an interest to understand the nature of the species stabilizing the nanoparticles. An understanding of the reduction and subsequent functionalization mechanism is necessary for a better comprehension of the properties of nanoparticles. The most common stabilizing agents used in gold nanoparticle synthesis are alkanethiols (Brust et al., 1994). One of the initial reports of gold nanoparticles synthesis employing hydroxylamine as the reducing agent triggered extensive use of organic amines as reducing and capping agents for the synthesis of gold nanoparticles (Graf & van Blaaderen, 2002).

Leff et al. (1996) succeeded in synthesizing hydrophobic gold nanocrystals functionalized with primary amines. Recently, Selvakannan et al. (2003) reported a water-soluble gold nanoparticle, functionalized with amino acid, lysine. Aslam et al. (2004) have also reported a one-step synthesis of oleyl amine-capped gold nanoparticles. A variety of other amino compounds have been experimented with as capping agents for gold nanoparticles. Thomas et al. used aminomethyl pyrene (2000) and benzylamine (2002) as stabilizing agents for gold nanoparticles. Kumar et al. (2003) have investigated the formation of complexes between alkylamines and gold nanoparticles. There have also been reports of aniline being used as reducing and capping agent (Nakao et al., 2003; Pillalamarri et al., 2004). Of late,

polyamidoamine (PAMAM) class of dendrimers have been used to incorporate auric ions, followed by their reduction leading to gold nanoparticles of 2–5 nm size (Wang et al., 2001). The exact nature of binding is still unknown. The N atom, the C=O moiety, and even the conjugated six-membered ring may all be potential binders on the metal surface. The weak signals from such interactions make it difficult to clearly establish the dendron coordination mode. The advantage of using an amine capping is that it lends itself to a variety of spectroscopic studies and thus the chemistry occurring at the surface of the nanoparticle can be probed easily. However, the exact mechanism of the reduction of auric ions and the subsequent capping is still unknown and we proposed to study this in some detail. We have chosen 2-methyl aniline (MA) for this investigation. The choice of this amine arises from the fact that its polymerized forms have wide-ranging applications in the fabrication of devices such as electrochromic displays and pH-based sensors. We show that during nanoparticle synthesis amine polymerization occurs; while one part covers the nanoparticle surface, another part precipitates from the solution. The results have been confirmed using aniline as the reducing agent. This study is a continuation of our investigations of the structure and properties of monolayers (Mitra et al., 2002; Mukhopadhyay et al., 2003; Nair et al., 2004a,b; Pradeep et al., 2004; Sandhyarani & Pradeep, 2003) of protected metal nanoparticles (Eswaranand & Pradeep, 2002; Nair et al., 2003, 2004a,b; Patel et al., 2003; Tom et al., 2003).

Experimental

Materials

Chloroauric acid trihydrate ($\text{HAuCl}_4 \cdot 3\text{H}_2\text{O}$) was purchased from CDH. 2-methyl aniline (MA), benzylchloride and bromoform were purchased from Sigma Aldrich. Ethyl acetate, 2-propanol and acetonitrile were purchased from local sources and distilled prior to use. 2-methyl aniline was vacuum-distilled prior to use. All other chemicals were used as such without further purification. Triply distilled de-ionized water was used for all the experiments. Potassium bromide (spectroscopic grade) used for infrared studies was purchased from Merck.

4-hydroxy azo benzoic acid was used as the matrix for Matrix Assisted Laser Desorption Ionization (MALDI) mass spectrometry studies and was purchased from Sigma Aldrich.

(1) *Synthesis of 2-methyl aniline – capped gold nanoparticles*: For the synthesis of 2-methyl aniline-capped gold nanoparticles (MA-AuNPs), 25 ml of 0.03% (by weight) aqueous solution of chloroauric acid trihydrate was heated to 80°C followed by the addition of 0.5 ml of 0.1 M aqueous MA. The reactants were stirred continuously for 20 min at the same temperature resulting in the formation of MA-AuNPs.

(2) *Purification*: For purification, the as-synthesized gold nanoparticles in the aqueous phase were mixed with ethyl acetate and shaken vigorously in a separating funnel. The nanoparticles were transferred into the organic layer, while the ionic impurities remained in the aqueous phase. Complete transfer of MA-AuNPs occurred. This is explained as due to the increased hydrophobicity of the capping agent with the incorporation of the methyl group. In addition, a bluish black precipitate was collected at the organic–aqueous junction. The organic portion containing the nanoparticles was centrifuged to recover the precipitate, which was analyzed by infrared spectroscopy and MALDI-TOF MS. The nanoparticles remained in the solution.

Nanoparticles in the organic phase were further concentrated using a rotavapor (Büchi rotavapor R-200) and dried under vacuum at room temperature to remove the unreacted parent organic compounds. The dried nanoparticles were found to be redispersible in organic solvents such as acetonitrile, tetrahydrofuran and ethyl acetate. All the studies were done with this purified material.

(3) *Estimation of gold and the polymer*: A known weight of the vacuum-dried MA-AuNPs was taken in a porcelain crucible and heated gradually to 700°C in a furnace held at atmospheric conditions (and cooled back to room temperature in air). The molecular cover was evaporated leaving behind a film of gold. From the known weight of gold film left behind and the initial weight of the nanoparticles taken, the monolayer quantity was estimated. Experiments of this kind were done using thermogravimetry also. From the weight loss measurements, an estimate of the fraction of total polymer formed, which goes to cap the gold nanoparticle is calculated.

(4) *Characterization*: Samples were characterized using UV–Visible spectroscopy (Perkin Elmer Lambda 25). Bright-field transmission electron microscope images were taken using a JEOL 3010 high-resolution transmission electron microscope (HRTEM) operated at 300 keV. The samples for transmission electron microscopy were prepared by dropping a dispersion of the particles on copper grid supported Formvar films. For recording infrared spectra, the vacuum-dried samples were made in the form of 1% (by weight) KBr pellets and the spectra were measured with a Perkin Elmer Spectrum One FT–IR spectrometer. Mass spectrometric studies were conducted using a Voyager DE PRO Biospectrometry Workstation of Applied Biosystems (MALDI-TOF MS). A pulsed nitrogen laser of 337 nm was used (maximum firing rate: 20 Hz, maximum pulse energy: 300 μ J) for the MALDI MS studies. The mass spectra were collected in both the negative and positive ion modes and were averaged for 100 shots. Nuclear magnetic resonance spectra of ^1H were recorded with a Bruker WM 400 spectrometer operating at 400 MHz (for ^1H). For this study, the vacuum-dried samples were redispersed in CD_3CN and the chemical shifts were measured with tetramethyl silane (TMS) as the reference. Thermal analysis was performed by Netsch STA 409 under nitrogen atmosphere. A scan rate of $10^\circ\text{C}/\text{min}$ was used.

Results and discussion

UV–Visible spectrum of MA-AuNPs in ethyl acetate is shown in Figure 1. The MA-AuNPs (Figure 1) exhibit a plasmon resonance peak at 530 nm. The slight red shift in λ_{max} when compared to Au@citrate in water arises from the large dielectric constant of the capping medium around the gold nanoparticles. The oxidized amine capping around the gold nanoparticles results in a positive charge on the surface of the nanoparticles. The λ_{max} was shifted to longer wavelengths as the amount of MA used in the synthesis was increased. A shift in the peak maximum with increase in amine concentration used in the synthesis suggests that more amine is incorporated onto the nanoparticle, increasing the shell thickness. This will not happen if amine exists on the surface of the nanoparticle as a monolayer of molecules as in the

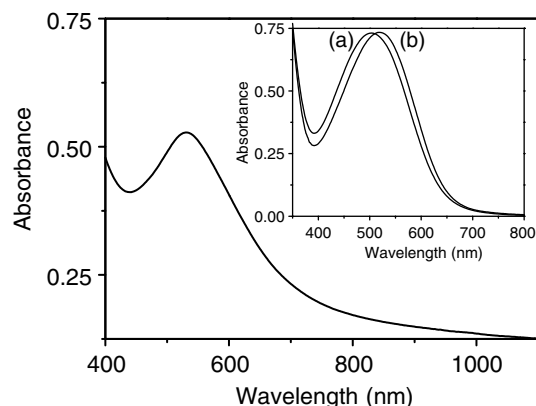


Figure 1. UV–Visible spectrum of MA-AuNPs taken with ethyl acetate as the solvent. Inset: UV–Visible spectra of MA-AuNPs synthesized with varying amounts of MA. 25 ml of 0.03% chloroauric acid was treated with 0.25 ml (a) and 0.375 ml (b) of MA giving a λ_{max} of 500 and 520 nm, respectively.

case of thiols (Sandhyarani & Pradeep, 2003). Although an increase in size of the nanoparticle can make this happen, the nanoparticle size is expected to decrease with increasing capping agent concentration (Hostetler et al., 1998).

A bright field transmission electron microscopy image (TEM) and an electron diffraction pattern of MA-AuNPs are shown in Figure 2. The formation of nanoparticles is clear from the TEM image. The mean diameter of the gold core as observed from the TEM images is 20 nm. A large area image (Figure 2d) fails to show the details, but an image of one particle (shown as Figure 2) shows a clear shell (of 5 nm thickness) and a core. The core is shown to be nanocrystalline gold (Figure 2c). Near spherical geometry was noticed for most of the particles. The TEM image suggests the possibility of a nearly homogeneous polymeric coating on the nanoparticle surface (see below).

To check the thickness and the porosity of the shell, the MA-AuNPs in ethyl acetate were treated separately with benzylchloride, sodium cyanide and bromoform in presence of isopropyl alcohol. As there was no reaction at room temperature, the solution was refluxed for 24 h. In the case of Au@citrate, the benzylchloride reaction leads to the mineralization of the core producing Au^{3+} within a few hours (Nair et al., 2003). In the present case, the reaction does not occur even under reflux conditions. However, irradiating the

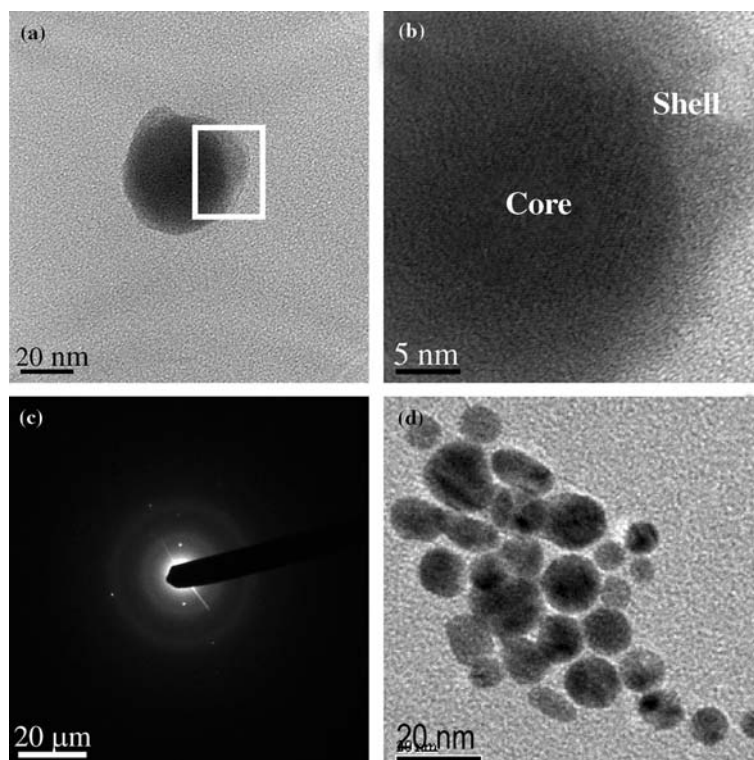


Figure 2. (a) TEM image of a single MA-AuNP having a clear demarcation between the core and the shell. Inset shows a larger area image giving well-separated MA-AuNPs. The portion enclosed by the box is magnified (45X) and shown in (b). (c) The electron diffraction pattern of the MA-AuNPs. (d) TEM image of a group of MA-AuNPs showing almost uniform size distribution and spherical shape.

reaction mixture containing bromoform with ultraviolet light (from a Xe arc lamp, 1 kW) brought about complete mineralization of the gold nanoparticles within 5 min. This reaction was monitored through UV-Visible spectrophotometry and the decrease in the surface plasmon resonance of the MA-AuNPs was accompanied by a simultaneous increase in a new peak at 398 nm indicative of the formation of Au^{3+} ion. Obviously, the radicals formed by photolysis of CHBr_3 do penetrate the shell. This observation supports a polymeric cover rather than an amine monolayer, the latter would have made the reaction with benzylchloride possible.

To arrive at the exact nature of the oxidized amine capping the gold nanoparticle and to investigate the capping mechanism, various studies such as infrared spectroscopy, ^1H NMR and MALDI-TOF MS studies were carried out on the vacuum-dried MA-AuNPs and the precipitate obtained during phase transfer.

The infrared (IR) spectrum of MA-AuNPs is compared with the corresponding pure aromatic amine in Figure 3. In the case of pure MA (Figure 3, curve a), the characteristic N-H symmetric and asymmetric absorption bands occur at 3370 and 3458 cm^{-1} , respectively. The corresponding regions in the case of MA-AuNPs (Figure 3, curve b) are broadened. The oxidized MA-AuNPs appears to form a polymeric network and broadening at 3450 cm^{-1} is ascribed to the presence of quinonoid ring forms. This is further supported by other features of the IR spectrum, which show marked decrease in intensity of the ring modes, due to the oxidation of MA. Quinonoid structures are known to show less intense bands at 1500 cm^{-1} than the benzenoid rings (Andrade et al., 1996).

The band at 1500 cm^{-1} decreases in intensity as MA is oxidized. This indicates the polymeric nature of the capping species. The argument that the gold nanoparticle is covered with a polymeric oxidized form of MA is further supported by the

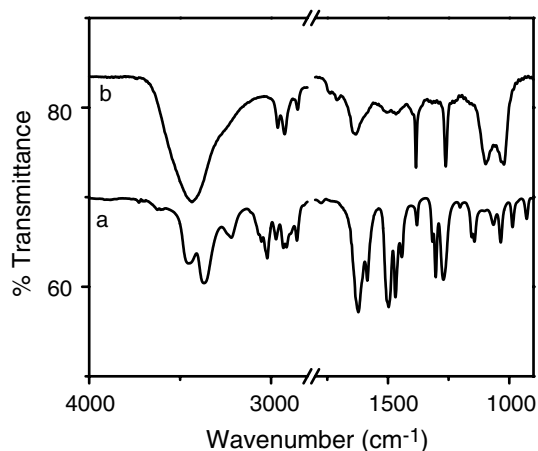


Figure 3. The infrared spectra of pure MA (curve a) and MA-AuNPs (curve b). The region from 2800 to 1800 cm^{-1} is featureless and therefore, not shown.

fact that the C=N stretching frequency, usually at 1600 cm^{-1} , shifts to lower wavenumbers and occurs as a shoulder at 1570 cm^{-1} . This is because of the presence of C-NH⁺=C group, which causes deformation of the bonds of the group (Andrade et al., 1996). The CH₃ deformation band at 1384 cm^{-1} is present which is manifested in the monomer also.

From these data, it is clear that the gold core is capped with a polymeric network of oxidized aromatic amines comprising of a mixture of benzenoid and quinonoid moieties. This is further substantiated by MALDI-TOF MS analysis. Mass spectrometric analysis of the nanoparticles in the positive ion mode shows well-resolved peaks with uniform separation of 105 Da in the case of MA-AuNPs, corresponding to C₇H₇N (Figure 4). The same sample when analyzed through the negative mode gave no distinct polymer peaks. Most of the peaks in the negative mode are

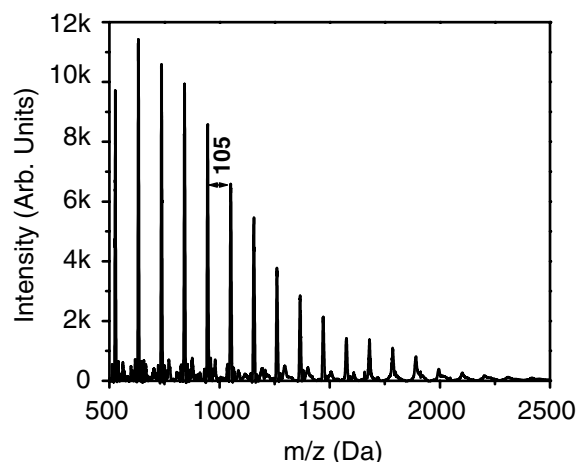


Figure 4. MALDI-TOF MS of MA-AuNPs taken in the linear positive mode. The sample was analyzed with 4-hydroxy azobenzoic acid (HABA) as the matrix.

attributed to the matrix. We conclude that it is because of the oxidized aromatic amine network (poly(2-methyl aniline)) present on the nanoparticle surface.

A post source decay (PSD) mass spectrum of the peak at m/z of 736 Da was measured in the reflectron analyzer, in the positive mode. Figure 5 shows the resultant spectrum showing peaks at m/z 526, 421, 316 and 211 and associated other ions, separated at m/z 105. PSD is not the best fragmentation mode and therefore, an ideal daughter ion spectrum is not obtained. However, polymeric nature of the ions is established.

The ¹H NMR spectrum of pure MA-AuNPs was recorded. In the ¹H-NMR of pure MA-AuNPs, it is observed that the methyl protons are shifted downfield to $\delta \sim 3$ ppm and the aromatic region possesses multiplet peak structure at $\delta \sim 7$ ppm. The signals in the ¹H NMR of MA-AuNPs are broadened because of spin-spin

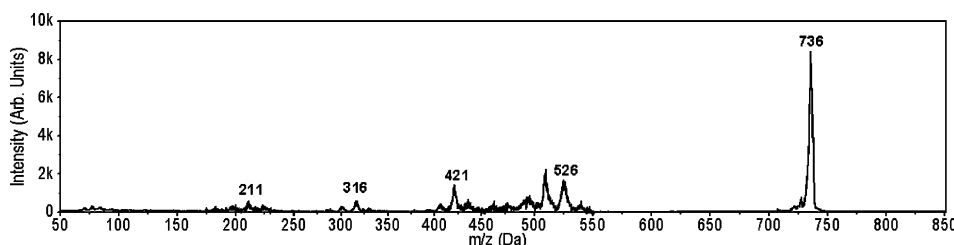


Figure 5. PSD mass spectrum of the peak at 736 Da shown in Figure 4.

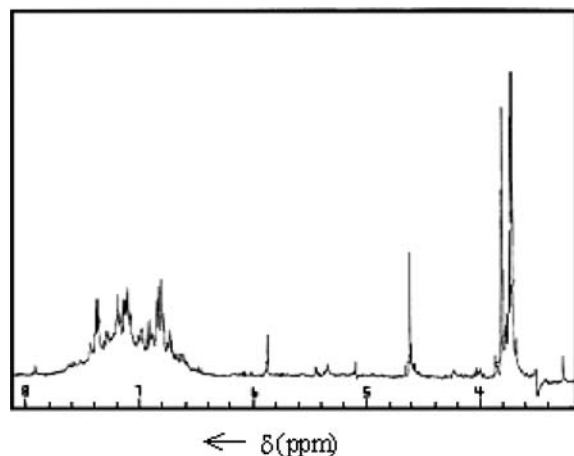


Figure 6. ^1H nuclear magnetic resonance spectrum of MA-AuNPs. The spectrum were collected with acetonitrile – $d_3(\text{CD}_3\text{CN})$ as the solvent and tetramethyl silane (TMS) as the reference.

relaxational (T_2) broadening (Figure 6). These features are indicative of the polymeric network associated with the gold nanoparticle.

The bluish black precipitate obtained during the purification of the nanoparticles was analyzed by infrared spectroscopy (Figure 7a). A notable feature in the infrared spectrum was the intense background absorption, starting at 1000 cm^{-1} and increasing up to 4000 cm^{-1} . This feature has been observed in polyaniline and is attributed to the presence of delocalized electrons (Colombian et al., 1994). As discussed in the case of MA-AuNPs, the appearance of a broad band at 3450 cm^{-1} , marked decrease in intensity of the peak at 1500 cm^{-1} due to contribution from quinonoid forms, the broad band at 1588 cm^{-1} and the prominent CH_3 deformation are all present in the IR spectrum of the residue. Therefore, it is concluded that the unreacted parent MA is polymerized in the presence of protons from chloroauric acid. The pH of the reaction mixture was acidic ($\text{pH} = 3.4$) at the start of the reaction, which aided polymerization. Analysis of the residue by MALDI-TOF MS (Figure 7b) further confirmed that the material is the polymer. The peaks spaced are spaced at m/z 105, just as in the case of Figure 4.

Based on the previously discussed experimental observations and spectroscopic evidences, we propose the following process for the formation of aromatic amine-capped gold nanoparticles from

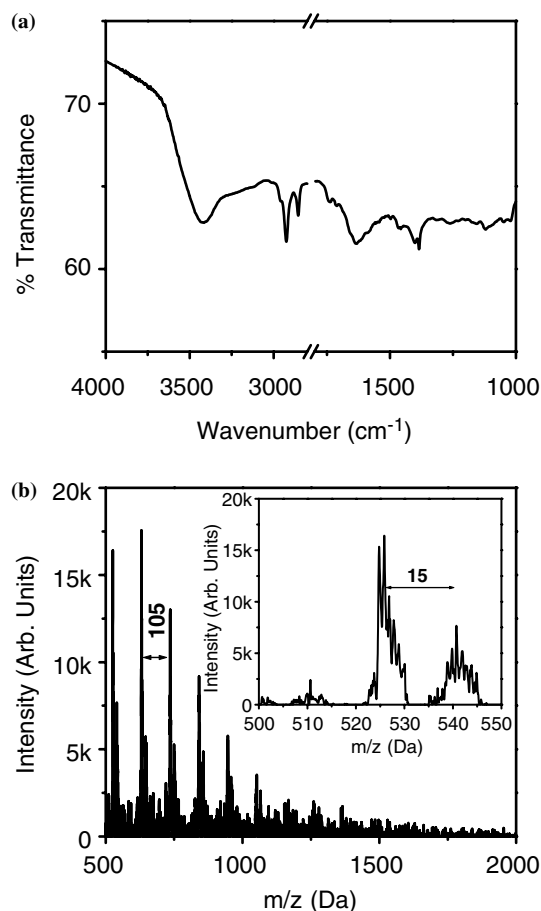
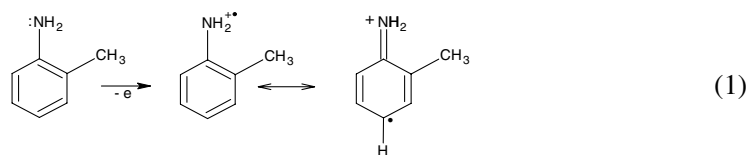
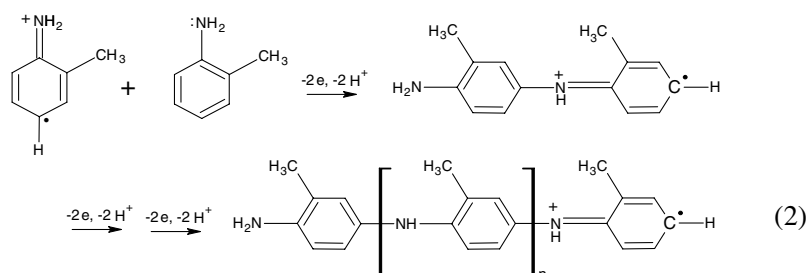
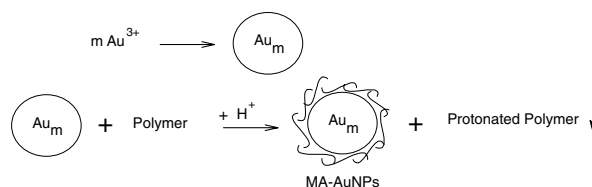
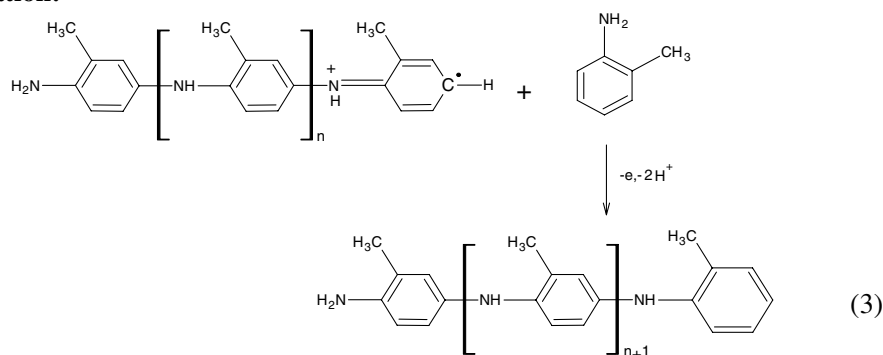


Figure 7. (a) Infrared spectrum and (b) MALDI-TOF MS of the residue obtained during phase transfer of MA-AuNPs. Inset of (b) shows an expanded region, where the second set of peaks differing by 15 Da from the original peaks is seen. The MALDI-TOF MS spectrum was recorded in the linear positive mode with sinapinic acid as the matrix. The spectrum was better with this matrix than with HABA.

auric ions. As shown in Scheme 1, the oxidation of the aromatic amine proceeds through the loss of electrons (Liu & Freund, 1997). The electrons formed go on to reduce the auric ions to gold atoms. The gold cluster formation and polymerization of the aromatic amine advance simultaneously. The polymer forms a shell around the gold nanoparticles, the process being favored by the strong affinity of gold towards the nitrogen atom. Some of the protons formed in the medium are taken up by a fraction of the polymer leading to its precipitation. These protons are likely to be

Initiation:**Propagation:****Termination:**

Scheme 1.

incorporated at the imine positions. This suggestion is supported by the MALDI spectrum given in Figure 7, which shows an additional set of peaks (in comparison to the spectrum presented in Figure 4) at 15 Da higher than the main peak (inset). This additional set occurs due to an addition of $-\text{NH}$ fragment to $\text{C}_7\text{H}_7\text{N}$ resulting in $\text{C}_7\text{H}_8\text{N}_2$ (which is likely to be $-\text{NH}-\text{C}_6\text{H}_3-\text{CH}_3\text{NH}-$). Fragmentation leading to this unit becomes possible due to protonation of the imine nitrogen of the polymeric chain. As the MA-AuNPs did not show this feature it is clear that most of the

polymeric capping on the nanoparticle is unprotonated. This may be expected as the nitrogens of the capping polymer are already involved in binding with the nanoparticle. Protonation of the polymeric chain is also evidenced by the unit mass spacing of all the peaks as shown in the inset of Figure 7b. Increase in the amine concentration results in a fractional increase in both the surface coverage and the polymeric precipitate. This was checked by an independent experiment. The process is summarized in Scheme 1. Increase in the concentration of H^+ was manifested in

terms of the decrease in pH during the course of the reaction (from 3.4 to 2.0). Based on the weight loss and thermogravimetry data, in a typical synthesis around 60% of the total polymer formed goes into capping the gold nanoparticle, while the remaining 40% is recovered as the polymeric precipitate.

Conclusion

Gold nanoparticle protected with poly(2-methyl aniline) were synthesized and characterized by various spectroscopic techniques. The process of reduction of the auric precursor and subsequent capping of the nanoparticles by the amines is elucidated. The reduction of the auric ions and the oxidation of the aromatic amine occur simultaneously, suggesting that they behave as a redox couple. It is found that the oxidative polymerization of the aromatic amines goes in step with the formation of gold nanoparticles from the reduced gold atoms. Finally the polymerized amine encapsulates the gold nanoparticle forming a robust shell. The polymer-protected nanoparticles were found to be inert towards mineralizing agents such as chloroform, bromoform, sodium cyanide and benzylchloride, which have been known to react with naked and monolayer-protected gold core.

Acknowledgements

T. P. acknowledges financial support from the Department of Science and Technology and Ministry of Information Technology for his research program on nanomaterials. C. S. and R.T.T thank the CSIR for research fellowships.

References

- Andrade E.M., F.V. Moline, M.I. Florit & D. Posadas, 1996. IR response of poly(o-toluidine): Spectral modifications upon redox state change. *Electroanal. Chem.* 419, 15–21.
- Aslam M., L. Fu, M. Su, K. Vijayamohan & V.P. Dravid, 2004. Novel one-step synthesis of amine-stabilized aqueous colloidal gold nanoparticles. *J. Mater. Chem.* 14, 1795–1797.
- Brust M., M. Walker, D. Bethell, D.J. Schiffrin & R. Whyman, 1994. Synthesis of thiol-derivatized gold nanoparticle in a two-phase liquid–liquid system. *J. Chem. Soc. Chem. Commun.* 7, 801–802.
- Colombian P., A. Gruger, A. Novak & A. Regis, 1994. Infrared and Raman study of polyaniline Part I. Hydrogen bonding and electronic mobility in emeraldine salts. *J. Mol. Struct.* 317, 261–266.
- Eswaranand V. & T. Pradeep, 2002. Zirconia protected silver clusters through functionalised monolayers. *J. Mater. Chem.* 12, 2421–2425.
- Graf C. & A. van Blaaderen, 2002. Metallo-dielectric colloidal core–shell particles for photonic applications. *Langmuir* 18, 524–534.
- Hostetler M.J., J.E. Wingate, C.J. Zhong, J.E. Harris, R.W. Vachet, M.R. Clark, J.D. Londono, S.J. Green, J.J. Stokes, G.D. Wignall, G.L. Glish, M.D. Porter, N.D. Evans & R.W. Murray, 1998. Alkanethiolate gold cluster molecules with core diameters from 1.5 to 5.2 nm: Core and monolayer properties as a function of core size. *Langmuir* 14, 17–30.
- Kumar A., S. Mandal, P.R. Selvakannan, R. Pasricha, A.B. Mandale & M. Sastry, 2003. Investigation into the interaction between surface-bound alkylamines and gold nanoparticles. *Langmuir* 19, 6277–6282.
- Leff D.V., L. Brandt & J.R. Heath, 1996. Synthesis and characterization of hydrophobic, organically-soluble gold nanocrystals functionalized with primary amines. *Langmuir* 12, 4723–4730.
- Liu G. & M.S. Freund, 1997. New approach for the controlled cross-linking of polyaniline: Synthesis and characterization. *Macromolecules* 30, 5660–5665.
- Mitra S., B. Nair, T. Pradeep, P.S. Goyal & R. Mukhopadhyay, 2002. Alkyl chain dynamics in monolayer protected clusters (MPCs): A quasielastic neutron scattering investigation. *J. Phys. Chem. B* 106, 3960–3967.
- Mukhopadhyay R., S. Mitra, I. Tsukushi, S. Ikeda & T. Pradeep, 2003. Evolution of dynamical motions in monolayer protected metal clusters. *Chem. Phys.* 292, 223–227.
- Nair A.S., T. Pradeep & I. Maclaren, 2004a. An investigation of the structure of stearate monolayer on Au@ZrO₂ and Ag@ZrO₂ core–shell nanoparticles. *J. Mater. Chem.* DOI: 10.1039/b313850j.
- Nair A.S., V. Suryanarayanan, R.T. Tom & T. Pradeep, 2004b. Porosity of core shell nanoparticles. *J. Mater. Chem.* In press.
- Nair A.S., R.T. Tom, V. Suryanarayanan & T. Pradeep, 2003. ZrO₂ bubbles from core shell nanoparticles. *J. Mater. Chem.* 13, 297–300.
- Nair A.S. & T. Pradeep, 2003. Halocarbon mineralization and catalytic destruction by metal nanoparticles. *Curr. Sci.* 84, 1560–1564.
- Nakao H., H. Shiigi, Y. Yamamoto, S. Tokonami, T. Nagaoka, S. Sugiyama & T. Ohtani, 2003. Highly ordered assemblies of Au nanoparticles organized on DNA. *Nano Lett.* 10, 1391–1394.

- Patel H., S.K. Das, T. Sundararajan, A.S. Nair, B. George & T. Pradeep, 2003. Thermal conductivities of naked and monolayer protected metal nanoparticle based nanofluids: Manifestation of anomalous enhancement and chemical effects. *Appl. Phys. Lett.* 83, 2931–2933.
- Pillalamarri S.K., F.D. Blum & M.F. Bertino, 2004. Surface-initiated polyaniline-coated gold nanoparticles. Abstracts of Papers, 228th ACS National Meeting, Philadelphia, PA, United States, August 22–26, 2004.
- Pradeep T., S. Mitra, A.S. Nair & R. Mukhopadhyay, 2004. Dynamics of alkyl chains in monolayer protected Au and Ag clusters and silver thiolates: A comprehensive QENS investigation. *J. Phys. Chem. B* 108, 7012–7020.
- Sandhyarani N. & T. Pradeep, 2003. Towards understanding structure and phase transitions of self-assembled monolayers on two- and three-dimensional surfaces: An overview of current efforts. *Int. Rev. Phys. Chem.* 22, 221–262.
- Selvakannan P.R., S. Mandal, S. Phadtare, R. Pasricha & M. Sastry, 2003. Capping of gold nanoparticles by the amino acid lysine renders them water-dispersible. *Langmuir* 19, 3545–3549.
- Thomas K.G. & P.V. Kamat, 2000. Making gold nanoparticles glow: Enhanced emission from a surface-bound fluoroprobe. *J. Am. Chem. Soc.* 122, 2655–2656.
- Thomas K.G., J. Zajicek & P.V. Kamat, 2002. Surface binding properties of tetraoctylammonium bromide-capped gold nanoparticles. *Langmuir* 18, 3722–3727.
- Tom R.T., A.S. Nair, N. Singh, M. Aslam, C.L. Nagendra, R. Philip, K. Vijayamohanan & T. Pradeep, 2003. Freely dispersible Au@TiO₂, Au@ZrO₂, Ag@TiO₂ and AgZrO₂ core-shell nano particles: One step synthesis, characterization, spectroscopy and optical limiting properties. *Langmuir* 19, 3439–3445.
- Wang R. J. Yang, Z. Zheng, M.D. Carducci, J. Jiao & S. Seraphin, 2001. Dendron-controlled nucleation and growth of gold nanoparticles. *Angew. Chem.* 40, 549–551.